Supporting information

Ford KR, Harrington CA, St. Clair JB. Photoperiod cues and patterns of genetic variation limit phenological responses to climate change in warm parts of species' range: modeling diameter-growth cessation in coast Douglas-fir.

Appendix S1. The beta-binomial model of diameter-growth cessation in autumn

We modeled the proportion of trees in a group (individuals from a particular physiographic subregion for a particular site and year) ceasing growth on a given day out of all the trees in that group growing prior to that day as a binomial process:

$$y_i \sim Binomial(n_i, \Pi_i) \qquad \text{S1.1}$$

Where y_i is the number of trees in a group observed ceasing growth on day i out of the n_i trees in that group growing prior to that day with probability Π_i. Each group j out of J total groups has m_j daily observations, for a total of M observations, with:

$$M = \sum_{j=1}^{J} m_j \qquad \text{S1.2}$$

Such that observations $i = 1, \ldots, M$ (i.e., "days" are group by day combinations). Π_i is Beta-distributed with parameters s_{1_i} and s_{2_i}:

$$\Pi_i \sim Beta(s_{1_i}, s_{2_i}) \qquad \text{S1.3}$$

$$s_{1_i} = \theta\pi_i \qquad \text{S1.4}$$

$$s_{2_i} = \theta(1 - \pi_i) \qquad \text{S1.5}$$

Where π_i is the daily probability of growth cessation in a particular group and θ is an overdispersion parameter. We defined the logit-transformed value of π_i as a linear function of environmental and seed-source variables:

$$logit(\pi_i) = a_{j[i]} + bP_i + cT_i + dP_iT_i + eA_i + fF_i \qquad \text{S1.6}$$

Where P_i is photoperiod and T_i is temperature on day i, A_i is mean actual evapotranspiration (AET) and F_i is mean frost exposure in the seed-source environments of all n_i trees in the group growing prior to day i, a_j is the value of the intercept of the linear function for group j, and b-f are the parameters characterizing the effects of the environmental and seed-source explanatory variables. Equation S1.6 is the "full" model. Candidate models were either this full model, or contained a subset of the full model's parameters (b-f) (Table 3, Table S2). All other aspects of

the candidate models were the same for each model. The intercept of the model (a_j) varies randomly by group according to a normal distribution:

$$a_j \sim Normal(\mu, \sigma_g) \qquad \text{S1.7}$$

Where μ is the mean value of the intercept across groups while σ_g is the standard deviation.

Appendix S2. Constraints imposed on model predictions

In our final fitted model of diameter-growth cessation in autumn, temperature and photoperiod exhibited negative effects on growth cessation probability (i.e., cessation was promoted by cool temperatures and short photoperiods) for the values of these variables that encapsulated the vast majority of the observed data (97.7%). However, due to the mathematical form of interaction effects in linear models, these effects will switch sign at some point in variable space. For our model, this sign switch affected the remaining 2.3% of the data, leading to predictions of a positive effect of temperature or a positive effect of photoperiod on cessation probability for this subset of the data. These biologically implausible effects occurred when either temperature or photoperiod fell below certain thresholds.

However, it is likely that the interaction effect that produced these switch points led to better fit in the variable space where most of the data fell, but worse fit outside that space. And because there was so much more data above the temperature and photoperiod thresholds where the switch points occur, the poor fit below the thresholds would not exert much influence on the optimized parameter values that produced these switch points. If these switch points were just model artifacts that do not reflect real biological mechanisms, they could produce misleading predictions when the model is applied to data outside the variable space occupied by the majority of the observed data. Thus, we decided to test the impact of constraining the model predictions so that the effects of temperature and photoperiod on growth cessation would be monotonic.

To explain these constraints, we first present the deterministic component of our final model:

$$logit(\pi) = \eta = a + bP + cT + dPT + fF \qquad \text{S2.1}$$

Where π is the probability of diameter-growth cessation, η is the linear predictor, P is photoperiod, T is temperature and F is frost exposure in the seed-source environment, while a, b, c, d and f are the parameters. We can identify where the switch points are located in variable space using the partial derivatives of η with respect to P and T. For example, if we take the partial derivative of η with respect to T and set that value to 0, the value of P will be P^*, the value of P where T switches from having a negative to positive effect on η:

$$\frac{\partial \eta}{\partial T} = c + dP \qquad \text{S2.2}$$

$$0 = c + dP^* \qquad \text{S2.3}$$

$$P^* = -\frac{c}{d} \qquad \text{S2.4}$$

Following the same reasoning, we can solve for T^*, the value of T where P switches from having a negative to positive effect on η:

$$\frac{\partial \eta}{\partial P} = b + dT \qquad \text{S2.5}$$

$$0 = b + dT^* \qquad \text{S2.6}$$

$$T^* = -\frac{b}{d} \qquad \text{S2.7}$$

The values of P^* and T^* also indicate what the value of η is when either $P = P^*$ or $T = T^*$ (or $P = P^*$ and $T = T^*$). We refer to this value as η^*:

$$\eta = a + bP + cT + dPT + fF \qquad \text{S2.8}$$

$$\begin{aligned} \eta^* &= a + bP^* + cT + dP^*T + fF = a + bP + cT^* + dPT^* + fF \\ &= a + bP^* + cT^* + dP^*T^* + fF \end{aligned} \qquad \text{S2.9}$$

$$\eta^* = a - \frac{bc}{d} + fF \qquad \text{S2.10}$$

For the constrained predictions, instead of using η as the value of the linear predictor, we use η_c, where:

$$\eta_c = \begin{cases} \eta; & if\ T \geq T^* \ \&\ P \geq P^* \\ \eta^*; & otherwise \end{cases} \qquad \text{S2.11}$$

Equation S2.11 shows that when the values of photoperiod and temperature are above the threshold values that result in the sign switch in η, the predicted value of η varies with photoperiod and temperature just like it would in the unconstrained predictions. But when the value of T or P falls below the corresponding threshold, the value of η is set to what it is at the thresholds. In our case, that means η_c increases as photoperiods get shorter and temperatures get cooler, but then saturates when it reaches a threshold value of photoperiod or temperature (P^* or T^*).

The constrained predictions actually led to a very slight improvement in root-mean-square error when comparing predictions and observations of the proportion of trees ceasing growth on each day (0.1011 versus 0.1016). This improvement was very small, but given there was any improvement over the unconstrained predictions and that the constrained predictions were more biologically plausible, we decided to use the constrained predictions.

The constraints on the predictions led to very few changes in the maps of predicted diameter-growth cessation dates in the autumn, and these changes were small. Under the current climate, the constraints led to a difference in predicted date of cessation in only 0.25% of map grid cells. In the grid cells with a difference between constrained and unconstrained predictions, the mean difference was 1.4 days and the maximum difference was 5 days. Under the future climate, no grid cells showed a difference in predicted cessation date between the constrained and unconstrained predictions. Therefore, while the constraints led to more biologically plausible and similarly accurate predictions, they had very little effect on our results and conclusions.

Table S1. The number of study trees and parent trees monitored for diameter-growth cessation from each physiographic subregion at each site in each year. For example, at the "cool" site in 2011, physiographic subregion "a" had 6 study trees that were monitored for diameter-growth cessation, and these trees were grown from seed that came from 4 different parent trees.

Site	Year	Physiographic subregion	Study trees	Parent trees
Cool	2011	a	6	4
Cool	2011	d	8	4
Cool	2012	a	9	4
Cool	2012	b	8	4
Cool	2012	d	7	5
Cool	2013	a	8	4
Cool	2013	b	7	4
Cool	2013	d	8	5
Cool	2014	a	3	3
Cool	2014	b	7	4
Cool	2014	d	8	5
Cool	2015	a	3	2
Cool	2015	b	4	4
Cool	2015	d	4	4
Intermediate	2010	a	8	4
Intermediate	2010	e	8	4
Intermediate	2011	a	9	5
Intermediate	2011	d	8	4
Intermediate	2011	e	6	3
Intermediate	2012	a	8	5
Intermediate	2012	b	8	4
Intermediate	2012	c	8	4
Intermediate	2012	d	6	4
Intermediate	2013	a	5	3
Intermediate	2013	b	3	3
Intermediate	2013	c	4	3
Intermediate	2013	d	2	2
Intermediate	2014	a	2	2
Intermediate	2014	b	2	2
Intermediate	2014	c	3	3
Intermediate	2014	d	3	3
Intermediate	2015	a	4	3
Intermediate	2015	b	4	3
Intermediate	2015	d	4	3
Warm	2010	a	8	4
Warm	2010	e	8	4
Warm	2011	a	8	4
Warm	2011	d	8	4

Table S1 (cont.).

Site	Year	Physiographic subregion	Study trees	Parent trees
Warm	2011	e	8	4
Warm	2012	a	7	4
Warm	2012	b	8	4
Warm	2012	d	7	4
Warm	2015	a	5	3
Warm	2015	b	5	4
Warm	2015	d	2	1

Table S2. Model parameter estimates for the corresponding explanatory variables (with 95% credible intervals) in the candidate generalized linear mixed effect models for diameter-growth cessation in autumn (same models as presented in Table 3 of the main text). We used the normalized values of the explanatory variables in model fitting ($x_{normalized} = (x - \bar{x})/sd_x$). The term "tempXphoto" refers to the interaction effect of temperature and photoperiod (using the normalized values of temperature and photoperiod). Model 1 was the final model used for subsequent analyses and predictions.

Model	Temperature	Photoperiod	tempXphoto	$\mathbf{Frost_{seed\text{-}source}}$	$\mathbf{AET_{seed\text{-}source}}$
1	-1.43 (-1.97, -0.91)	-2.54 (-3.02, -2.08)	-0.78 (-1.15, -0.43)	0.23 (0.03, 0.45)	-
2	-1.42 (-1.95, -0.88)	-2.55 (-3.05, -2.08)	-0.76 (-1.13, -0.42)	0.31 (0.00, 0.63)	0.09 (-0.19, 0.38)
3	-1.43 (-1.95, -0.91)	-2.49 (-2.98, -2.03)	-0.77 (-1.12, -0.43)	-	-
4	-1.44 (-1.97, -0.91)	-2.51 (-3.03, -2.06)	-0.79 (-1.15, -0.45)	-	-0.11 (-0.31, 0.07)
5	-0.38 (-0.61, -0.15)	-2.09 (-2.51, -1.70)	-	-	-
6	-	-2.51 (-2.86, -2.19)	-	-	-
7	-1.44 (-1.62, -1.28)	-	-	-	-
8	-	-	-	-	-

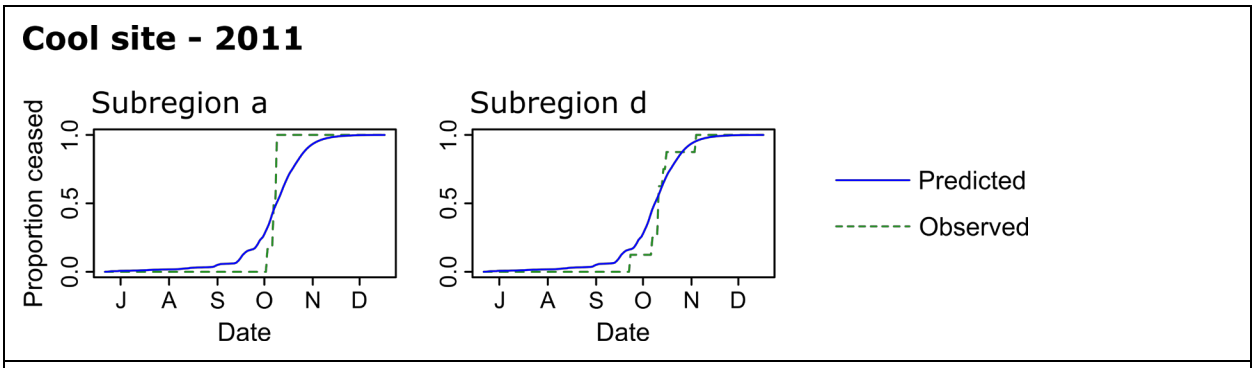

Fig. S1. Comparison of predicted and observed values of the proportion of trees that had ceased diameter growth over time for each seed-source physiographic subregion at the cool site in 2011, according to the autumn diameter-growth cessation pathway.

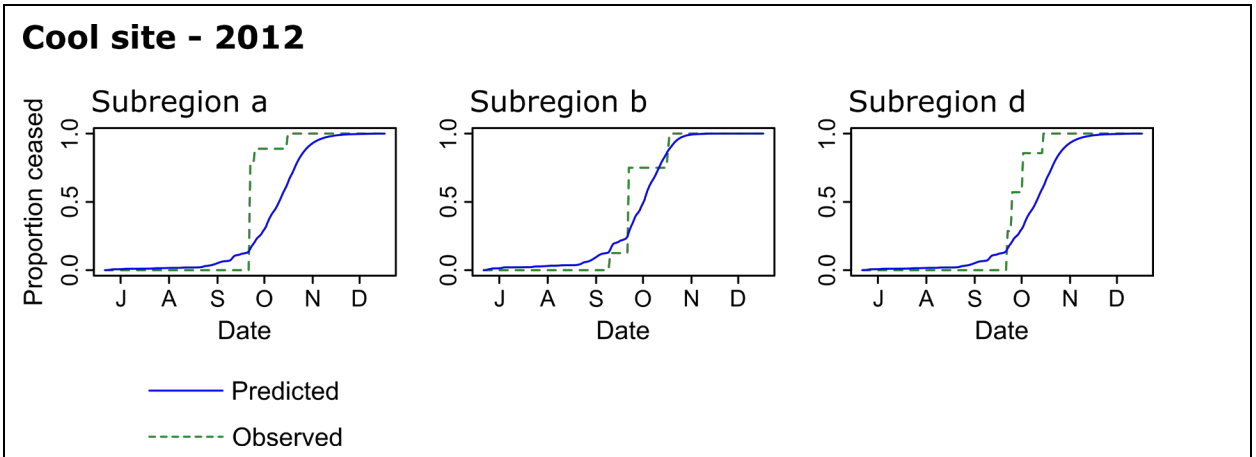

Fig. S2. Comparison of predicted and observed values of the proportion of trees that had ceased diameter growth over time for each seed-source physiographic subregion at the cool site in 2012, according to the autumn diameter-growth cessation pathway.

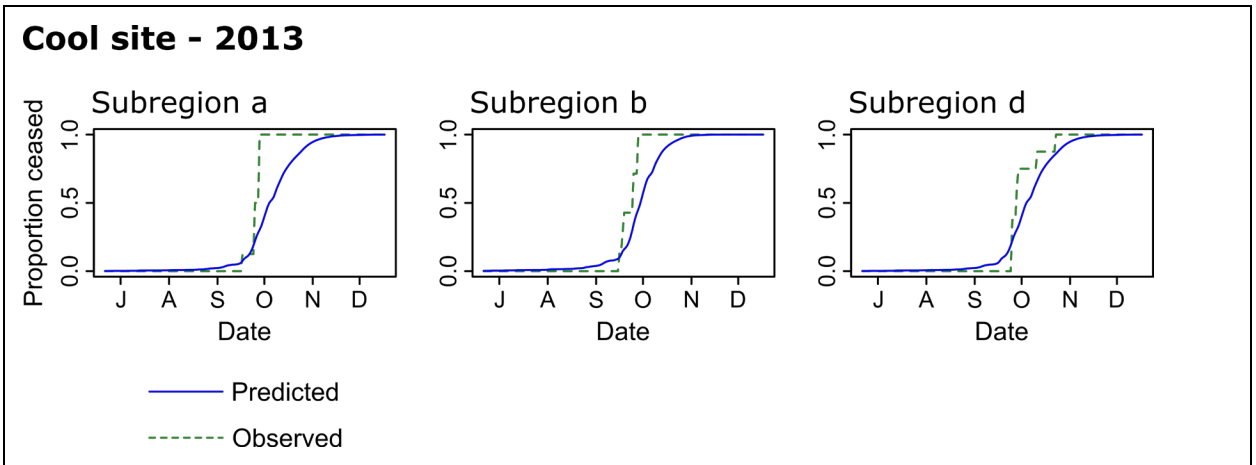

Fig. S3. Comparison of predicted and observed values of the proportion of trees that had ceased diameter growth over time for each seed-source physiographic subregion at the cool site in 2013, according to the autumn diameter-growth cessation pathway.

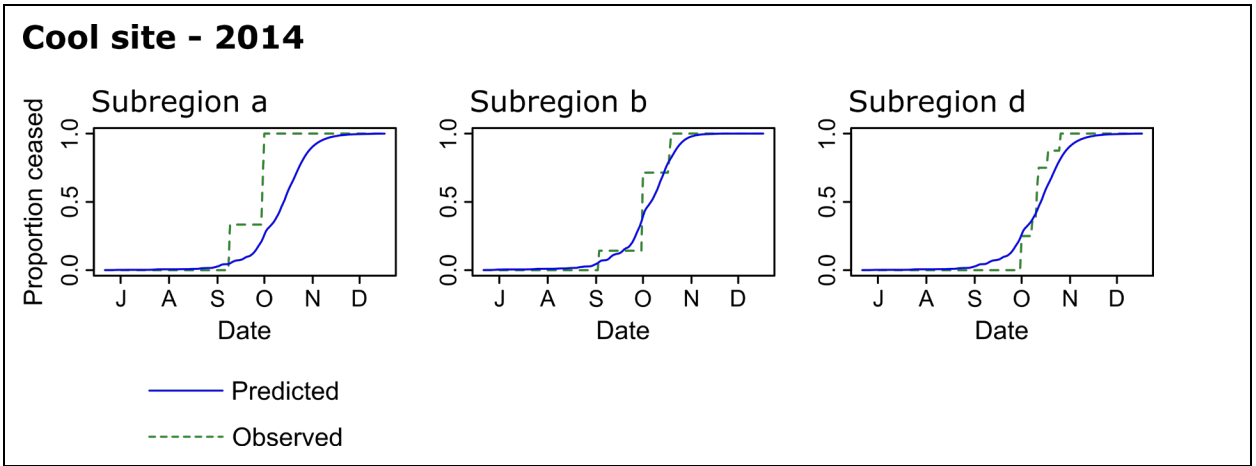

Fig. S4. Comparison of predicted and observed values of the proportion of trees that had ceased diameter growth over time for each seed-source physiographic subregion at the cool site in 2014, according to the autumn diameter-growth cessation pathway.

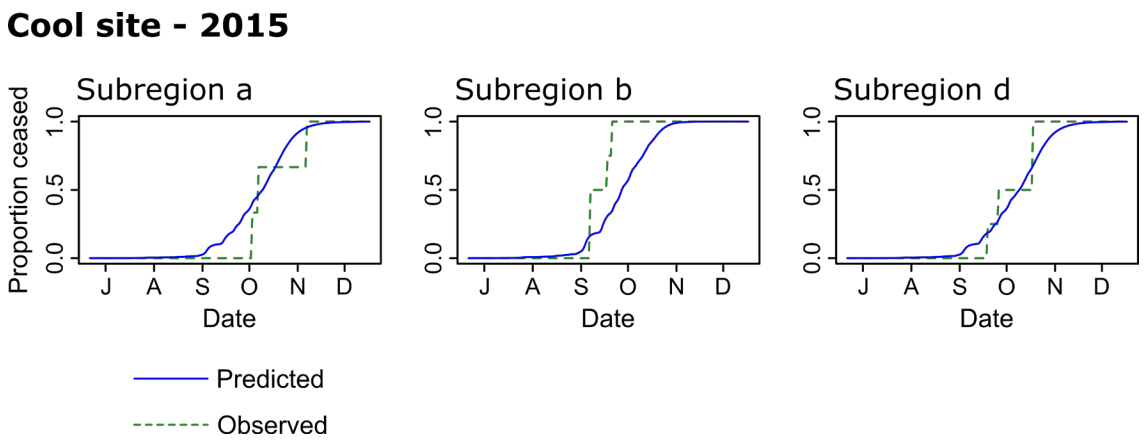

Fig. S5. Comparison of predicted and observed values of the proportion of trees that had ceased diameter growth over time for each seed-source physiographic subregion at the cool site in 2015, according to the autumn diameter-growth cessation pathway.

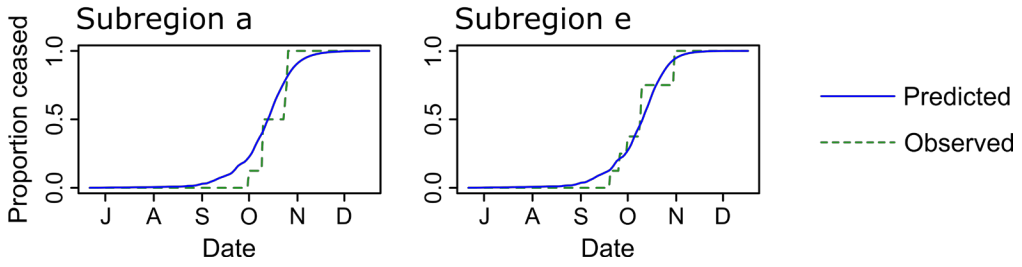

Fig. S6. Comparison of predicted and observed values of the proportion of trees that had ceased diameter growth over time for each seed-source physiographic subregion at the intermediate site in 2010, according to the autumn diameter-growth cessation pathway.

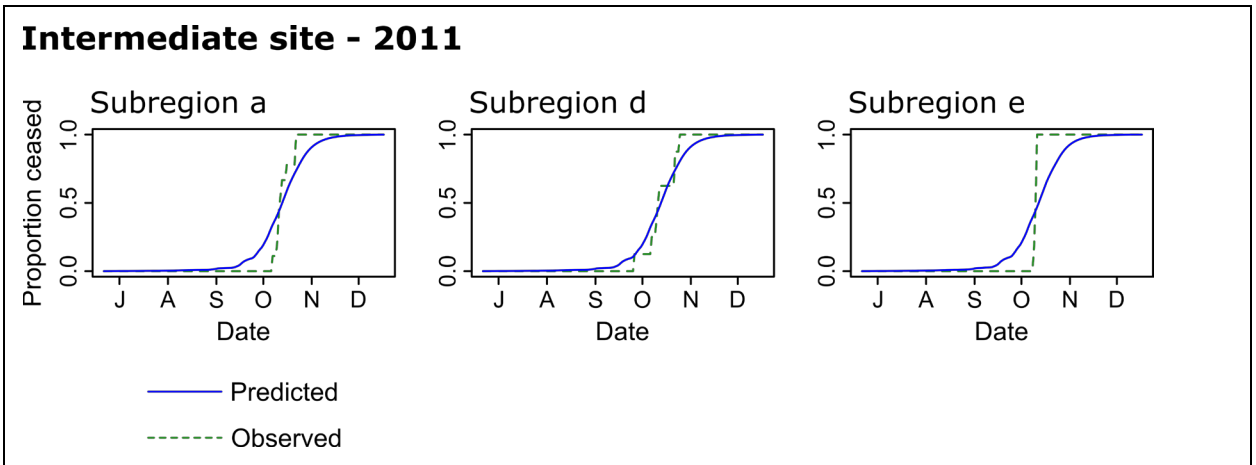

Fig. S7. Comparison of predicted and observed values of the proportion of trees that had ceased diameter growth over time for each seed-source physiographic subregion at the intermediate site in 2011, according to the autumn diameter-growth cessation pathway.

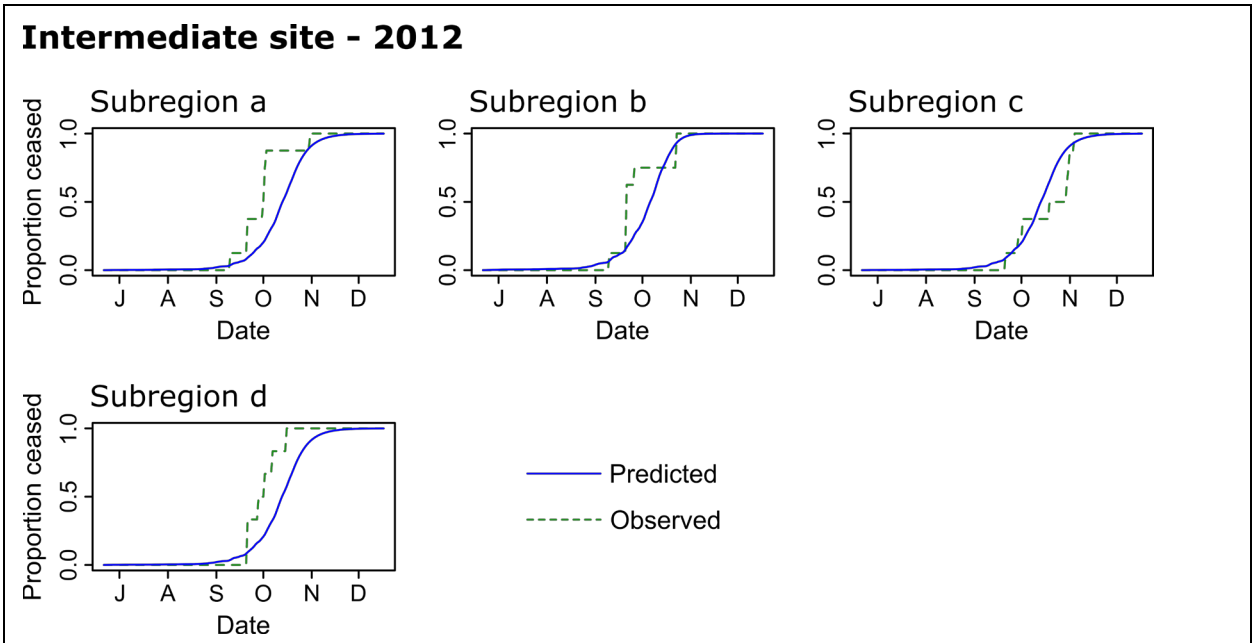

Fig. S8. Comparison of predicted and observed values of the proportion of trees that had ceased diameter growth over time for each seed-source physiographic subregion at the intermediate site in 2012, according to the autumn diameter-growth cessation pathway.

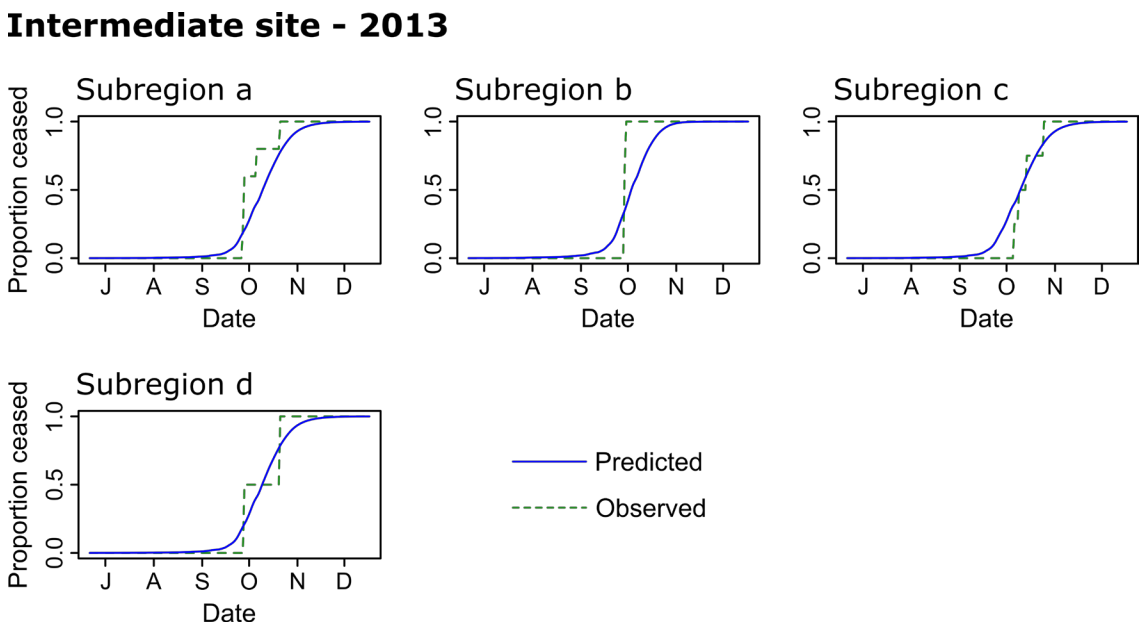

Fig. S9. Comparison of predicted and observed values of the proportion of trees that had ceased diameter growth over time for each seed-source physiographic subregion at the intermediate site in 2013, according to the autumn diameter-growth cessation pathway.

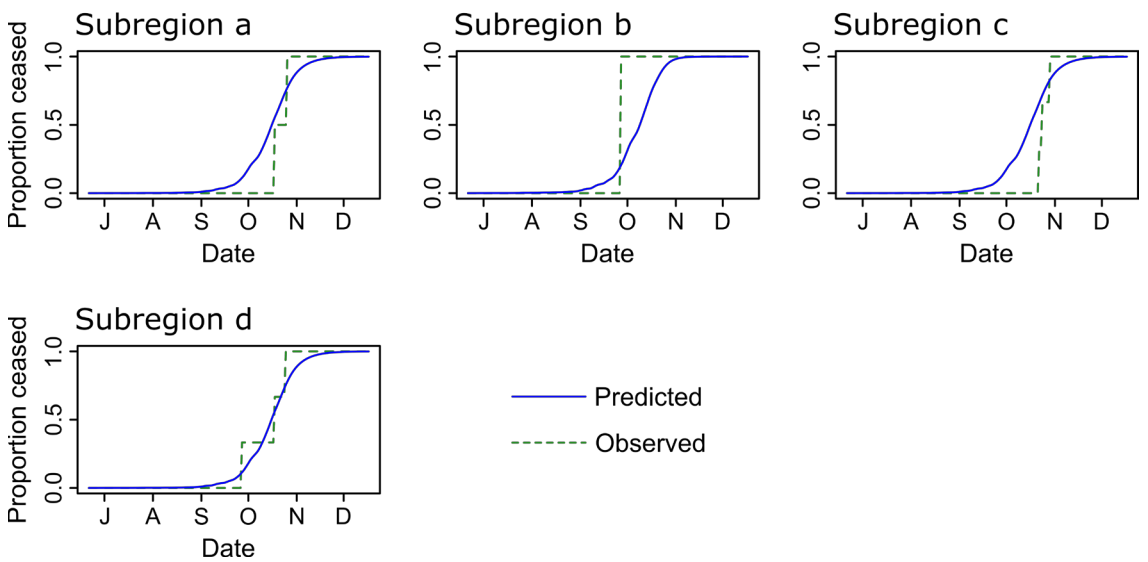

Fig. S10. Comparison of predicted and observed values of the proportion of trees that had ceased diameter growth over time for each seed-source physiographic subregion at the intermediate site in 2014, according to the autumn diameter-growth cessation pathway.

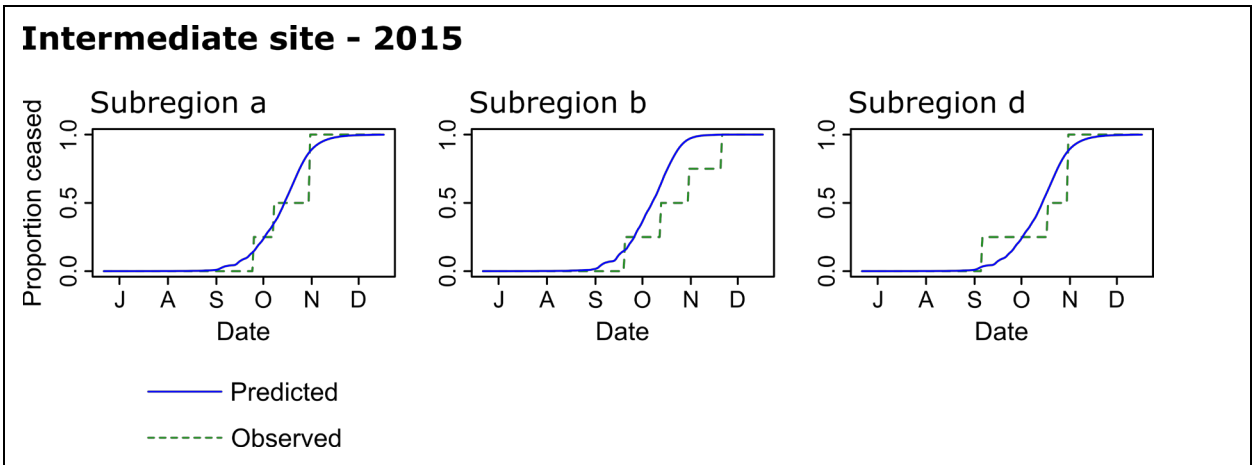

Fig. S11. Comparison of predicted and observed values of the proportion of trees that had ceased diameter growth over time for each seed-source physiographic subregion at the intermediate site in 2015, according to the autumn diameter-growth cessation pathway.

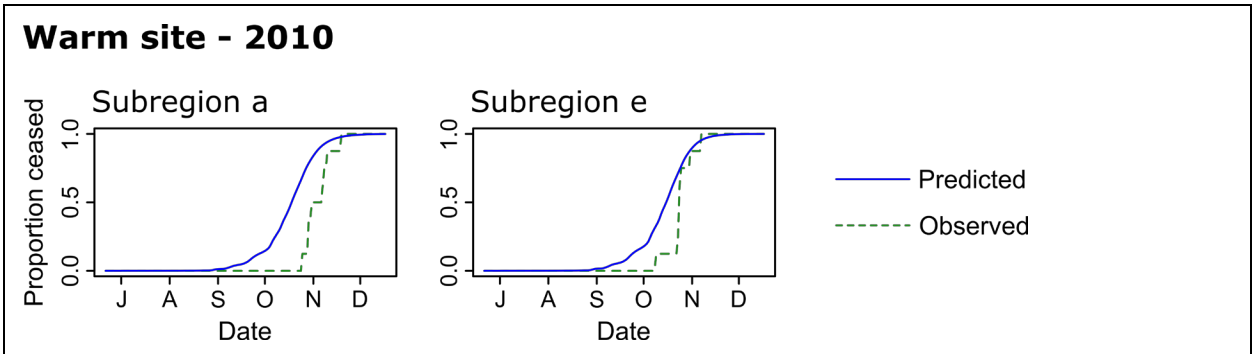

Fig. S12. Comparison of predicted and observed values of the proportion of trees that had ceased diameter growth over time for each seed-source physiographic subregion at the warm site in 2010, according to the autumn diameter-growth cessation pathway.

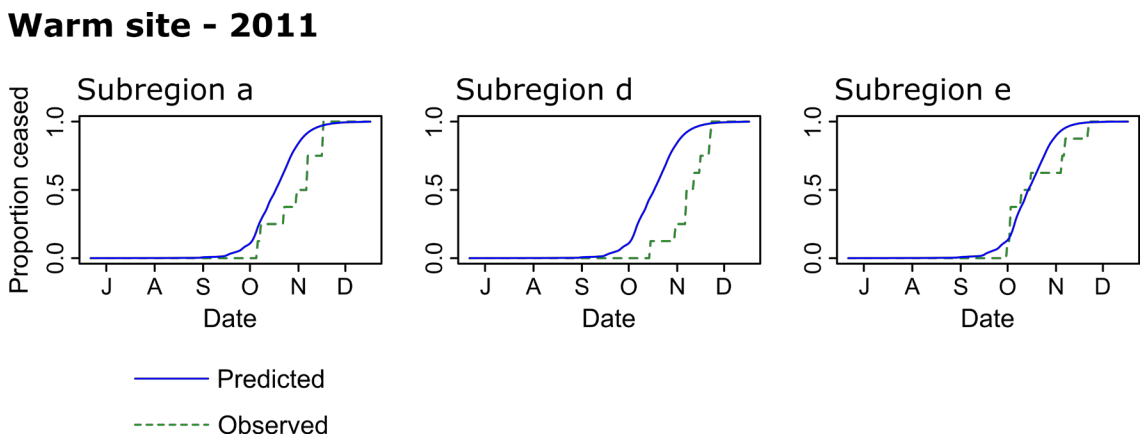

Fig. S13. Comparison of predicted and observed values of the proportion of trees that had ceased diameter growth over time for each seed-source physiographic subregion at the warm site in 2011, according to the autumn diameter-growth cessation pathway.

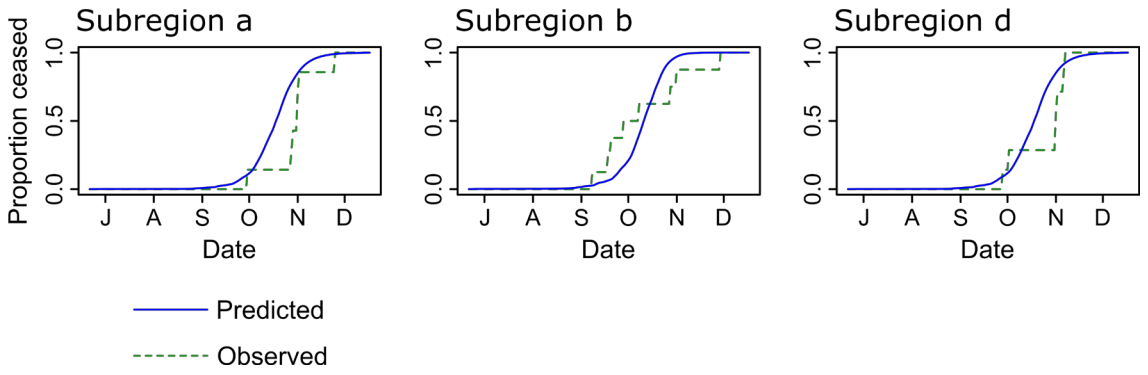

Fig. S14. Comparison of predicted and observed values of the proportion of trees that had ceased diameter growth over time for each seed-source physiographic subregion at the warm site in 2012, according to the autumn diameter-growth cessation pathway.